Check for updates

Molecular Plant Pathology

WILEY

ORIGINAL ARTICLE OPEN ACCESS

Integrated Functional Characterization of *Hemileia vastatrix* Effector Candidates Reveals Coordinated Immune Suppression, Sequential Deployment and Compartment-Specific Targeting

Thiago Maia[1,2] | Gustavo Marin-Ramirez[1,3] | Maicon N. Araujo[1] | Larissa G. Zanardo[1] | Sérgio H. Brommonschenkel[1]

[1]Department of Plant Pathology and National Institute for Plant-Pest Interactions/Institute of Biotechnology Applied to Agriculture (Bioagro), Federal University of Viçosa, Viçosa, Minas Gerais, Brazil | [2]Department of Plant Pathology and Center for Plant Science Innovation, University of Nebraska-Lincoln, Lincoln, Nebraska, USA | [3]Plant Pathology, National Center for Coffee Research (CENICAFÉ), Chinchiná, Caldas, Colombia

Correspondence: Sérgio H. Brommonschenkel (shbromo@ufv.br)

Received: 14 December 2025 | **Revised:** 17 August 2026 | **Accepted:** 25 August 2026

Keywords: biotrophy | coffee leaf rust | disease resistance | effector-triggered immunity | haustorium | pattern-triggered immunity | *SH* resistance | virulence

ABSTRACT

Coffee leaf rust, caused by the obligate biotrophic fungus *Hemileia vastatrix*, remains the most destructive disease of coffee worldwide. Although genomic and transcriptomic studies have identified a large number of candidate effectors, experimental evidence supporting their biological roles during infection remains limited. Here, we integrated functional assays, temporal expression profiling during coffee infection and subcellular localization analyses to investigate the biological properties of 44 *H. vastatrix* effector candidates (HvECs). Using the *Pseudomonas fluorescens* EtHAn effector delivery system in *Nicotiana benthamiana*, 15 HvECs consistently suppressed pattern-triggered immunity (PTI), indicating that immune suppression is a widespread property among the *H. vastatrix* effector repertoire, as assessed in this heterologous system. Five HvECs also attenuated AvrB-triggered effector-triggered immunity (ETI), and three suppressed both PTI and ETI, suggesting that a subset of HvECs targets conserved regulatory nodes shared by these interconnected immune pathways. Temporal expression profiling revealed sequential deployment of HvECs throughout infection, with distinct subsets predominating during pre-biotrophic development, host penetration or biotrophic colonization, consistent with stage-specific functions during fungal pathogenesis. Subcellular localization analyses further showed that HvECs preferentially accumulated in the nucleus or chloroplasts, compartments known as central hubs of plant immune regulation. This study provides the most comprehensive functional characterization of *H. vastatrix* effector candidates to date, establishes a biologically informed framework for prioritizing candidates for future identification of avirulence determinants recognized by *SH* resistance genes, and advances our understanding of how the coffee rust fungus orchestrates immune suppression across time and cellular space during pathogenesis.

This is an open access article under the terms of the Creative Commons Attribution-NonCommercial-NoDerivs License, which permits use and distribution in any medium, provided the original work is properly cited, the use is non-commercial and no modifications or adaptations are made.

© 2026 The Author(s). *Molecular Plant Pathology* published by British Society for Plant Pathology and John Wiley & Sons Ltd.

1 | Introduction

Coffee leaf rust (CLR), caused by the obligate biotrophic fungus *Hemileia vastatrix*, remains the most destructive disease of coffee worldwide and continues to threaten the durability of genetic resistance despite more than a century of research. Although resistant cultivars carrying *SH* resistance genes represent the most economical and sustainable strategy for disease management, the recurrent emergence of physiological races capable of overcoming most resistance sources highlights the remarkable adaptive potential of the pathogen and underscores the need to better understand the molecular mechanisms governing pathogenicity, host colonization and immune recognition (Cabral et al. 2009; Talhinhas et al. 2017; Sera et al. 2022; Silva et al. 2022; Brenes et al. 2025). As an obligate biotroph, *H. vastatrix* establishes prolonged interactions with living host cells through specialized haustoria, requiring continuous modulation of host physiology throughout a latent period that may extend for nearly one month (Maia, Badel, Fernandes, et al. 2017; Silva et al. 2002). This intimate association strongly suggests that successful colonization depends on the coordinated deployment of effector proteins that suppress host immunity while modulating cellular processes required to establish and maintain long-term biotrophy.

Effector proteins are widely recognized as central molecular components of the molecular machinery that enables pathogenesis in filamentous plant pathogens (Li et al. 2024). Although they manipulate a wide range of host cellular processes, suppression of plant immunity represents one of their most fundamental and best-characterized functions. Increasing evidence further indicates that effector activity is intimately associated with both their temporal deployment during infection and their localization within specific host cellular compartments, where they interact with distinct immune regulatory pathways (Petre et al. 2014; Rocafort et al. 2020; Ngou, Ding, and Jones 2022). Recent advances in comparative genomics, structural biology and artificial intelligence have dramatically expanded the discovery of candidate effectors (Jones and Raffaele 2025), shifting the field from candidate identification towards functional characterization. At the same time, subcellular localization has emerged as an important predictor of effector function because individual cellular compartments harbour specialized signalling networks involved in immune regulation. Likewise, temporal expression patterns provide an additional functional dimension, reflecting the dynamic deployment of effector repertoires during successive stages of host colonization. Because intracellular nucleotide-binding leucine-rich repeat (NLR) receptors perceive effector activities directly or indirectly through their effects on host targets (Ngou, Ding, and Jones 2022), identifying effectors that suppress immunity, are expressed at biologically relevant stages of infection, and localize to strategic host compartments provides a rational strategy for prioritizing candidates involved in virulence and *SH*-mediated resistance.

Although genomic and transcriptomic studies have identified multiple *H. vastatrix* candidate effectors expressed during coffee infection, particularly during the biotrophic phase (Fernandez et al. 2012; Talhinhas et al. 2014; Porto et al. 2019; Castro et al. 2022), experimental evidence supporting their biological functions remains extremely limited. To date, HvEC-016 is the only effector experimentally demonstrated that may function as an avirulence determinant recognized by coffee genotypes carrying the *SH1* resistance gene (Maia, Badel, Marin-Ramirez, et al. 2017). Consequently, the immune-suppressive activities, temporal deployment, intracellular localization and contribution to pathogenesis of the vast majority of predicted *H. vastatrix* effectors remain unknown. This disparity reflects a broader transition in effector biology, in which advances in candidate discovery have substantially outpaced experimental validation, making integrated functional characterization one of the principal challenges for understanding the molecular basis of pathogenesis and host adaptation.

Progress in addressing this knowledge gap for CLR has been constrained by major experimental limitations. The obligate biotrophic nature of *H. vastatrix* precludes stable genetic transformation and reverse-genetic analyses, while coffee still lacks robust, high-throughput transient expression systems suitable for large-scale functional studies, despite recent advances in *Agrobacterium*-mediated transformation of detached leaves (Vargas-Guevara et al. 2018). Consequently, heterologous experimental systems remain indispensable for investigating *H. vastatrix* effectors. Among these, the *Pseudomonas fluorescens* EtHAn effector delivery system provides a unique advantage because it retains a functional Type III secretion system while lacking endogenous bacterial effectors, allowing fungal effectors to be delivered into plant cells with minimal background interference (Thomas et al. 2009; Maia et al. 2022). Combined with the experimental versatility of *Nicotiana benthamiana*, whose conserved immune signalling pathways provide an effective platform for dissecting effector activities, this system enables high-throughput functional analyses of immune suppression while simultaneously facilitating studies of intracellular targeting.

We hypothesized that *H. vastatrix* deploys functionally distinct effector candidates in a coordinated manner throughout infection and that integrating immune-suppressive activity with temporal expression and subcellular localization would reveal how these effectors contribute to fungal pathogenesis while enabling the biologically informed prioritization of candidate effectors involved in *SH*-mediated immune recognition. To test this hypothesis, we functionally characterized a collection of previously predicted *H. vastatrix* effector candidates using the *P. fluorescens* EtHAn effector delivery system, evaluated their ability to suppress pattern-triggered immunity (PTI) and effector-triggered immunity (ETI), determined their expression profiles during coffee infection and investigated the subcellular localization of selected proteins. Collectively, these complementary analyses provide the first comprehensive functional characterization of a diverse repertoire of *H. vastatrix* effector candidates, revealing how immune suppression, temporal deployment and compartment-specific targeting are coordinated throughout fungal pathogenesis. Our study also establishes a biologically informed basis for prioritizing candidate effectors for future studies aimed at identifying avirulence determinants recognized by SH resistance proteins.

13643703, 2026, 9, Downloaded from https://bsppjournals.onlinelibrary.wiley.com/doi/10.1111/mpp.70341 by Cochrane Colombia, Wiley Online Library on [12/11/2026]. See the Terms and Conditions (https://onlinelibrary.wiley.com/terms-and-conditions) on Wiley Online Library for rules of use; OA articles are governed by the applicable Creative Commons License

2 | Results

2.1 | Functional Screening Identifies HvECs That Suppress PTI in a Heterologous *N. benthamiana* System

To identify *H. vastatrix* effector candidates (HvECs) capable of suppressing PTI, 44 candidates were individually delivered into *N. benthamiana* leaf cells using the *P. fluorescens* EtHAn (Pf EtHAn) effector delivery (EDV) system. In this assay, infiltration with the nonpathogenic Pf EtHAn strain activates PTI, which restricts the growth of the subsequently infiltrated pathogenic bacterium *Pseudomonas syringae* pv. *tomato* (Pto) DC3000, preventing its population from reaching the level required to deliver sufficient Type III effectors (T3Es) and thereby preventing the hypersensitive response (HR) (Figure 1a). Restoration of HR following HvEC delivery therefore indicates suppression of PTI (Crabill et al. 2010; Nguyen et al. 2010; Badel et al. 2013; Maia et al. 2022).

Among the 44 HvECs screened, 15 consistently suppressed PTI (HvEC_002, HvEC_004A, HvEC_005, HvEC_006, HvEC_016, HvEC_021, HvEC_028, HvEC_036, HvEC_040, HvEC_053, HvEC_056, HvEC_064, HvEC_071, HvEC_081 and HvEC_101), as evidenced by HR development at the intersection between the bacterial infiltration zones in ≥ 50% of infiltration sites, the threshold used to classify PTI suppressors (Figure 1b; Table S1). Twelve candidates exhibited strong suppressive activity, inducing HR in more than 83% of the tested infiltrated leaves, whereas three candidates displayed intermediate suppression frequencies ranging from 62.5% (HvEC_056) to 75% (HvEC_005 and HvEC_040) (Figure 1b). For each of these 15 HvECs, macroscopic tissue collapse consistent with HR was visible within the overlapping region of *N. benthamiana* leaves infiltrated with Pf EtHAn expressing the corresponding HvEC and subsequently with Pto DC3000, and this cell death was confirmed by trypan blue staining of the same tissue (Figure 1c). Candidates exhibiting suppression frequencies below 50% were considered non-suppressor in this assay. Overall, approximately one-third (34%) of the HvECs evaluated functioned as PTI suppressors, suggesting that immune suppression is a widespread property among candidate effectors of the predicted *H. vastatrix* repertoire, as assessed in this heterologous Pf EtHAn/*N. benthamiana* system.

To determine whether PTI suppression resulted in enhanced pathogen colonization, the 15 PTI-suppressing HvECs were further evaluated for their ability to promote multiplication of Pto DC3000 in *N. benthamiana*. Leaves were first infiltrated with Pf EtHAn expressing individual *HvEC*s and subsequently challenged with Pto DC3000. All 15 HvECs that suppressed PTI also promoted bacterial proliferation within the overlapping infiltration zones (Figure 2). The effect became evident at 24 h after Pto DC3000 inoculation and was most pronounced at 48 h, when bacterial populations exceeded those of the empty vector control by more than three orders of magnitude (Figure 2). By contrast, no detectable bacterial multiplication occurred in the negative control, indicating that PTI elicited by Pf EtHAn effectively restricted pathogen growth in the absence of HvEC-mediated immune suppression.

Together, these results demonstrate that a substantial proportion of the *H. vastatrix* effector repertoire can effectively suppress PTI when delivered via the Pf EtHAn system, with a clear biological consequence of enhanced Pto DC3000 proliferation.

2.2 | A Subset of HvECs Suppresses ETI

To determine whether *H. vastatrix* effectors also interfere with ETI, 20 HvECs, including the 15 PTI suppressors identified above and five additional candidates, were evaluated using an AvrB-induced hypersensitive response (HR) assay in *N. benthamiana* (Maia et al. 2022). Leaves were co-infiltrated with Pf EtHAn expressing AvrB and Pf EtHAn delivering individual HvECs at a 1:1 ratio, and HR development was evaluated 48 h after infiltration. As expected, Pf EtHAn expressing AvrB elicited a robust HR, whereas Pf EtHAn carrying the empty pEDV6 vector did not induce HR, confirming the specificity of the assay (Figure S1).

Five HvECs (HvEC_006, HvEC_032, HvEC_043, HvEC_053 and HvEC_081) consistently attenuated or suppressed AvrB-triggered HR in more than 50% of the tested leaves (Figure 3a; Table S2). HvEC_043 exhibited the strongest activity, suppressing HR in more than 70% of the infiltrated leaves, whereas HvEC_032 and HvEC_081 displayed intermediate suppression frequencies of 66.6% and 62.5%, respectively (Figure 3a). Notably, three of these candidates (HvEC_006, HvEC_053 and HvEC_081) also suppressed PTI (Figures 1 and 2), indicating that a subset of HvECs interferes with both major layers of plant innate immunity.

To quantitatively validate these observations, ion leakage associated with HR-associated membrane disruption was monitored between 0 and 28 h after infiltration. From 16 h onward, conductance values for AvrB co-expressed with each of the five HvECs remained consistently below the standard error range of the AvrB + empty vector control (Figure 3b), indicating a reduction in electrolyte leakage associated with each of these effectors and confirming that they attenuate ETI-associated cell death.

Together, these results identify five HvECs capable of suppressing ETI and reveal three multifunctional effectors that suppress both PTI and ETI, suggesting that they may target conserved components shared between the two immune pathways.

2.3 | HvECs Are Deployed at Distinct Stages of Coffee Infection

To determine when the identified immunosuppressive HvECs are deployed during infection, we examined the transcript accumulation of 17 *HvEC* genes throughout the *H. vastatrix* life cycle (Figure 4; Table 1). Ten expression profiles were previously reported (Maia, Badel, Marin-Ramirez, et al. 2017), whereas the remaining seven were determined here by reverse transcription-quantitative PCR (RT-qPCR).

The *HvEC*s displayed distinct temporal expression patterns that could be grouped according to the stage at which transcript accumulation reached its maximum (Figure 4). Four genes (*HvEC*_036, *HvEC*_040, *HvEC*_028 and *HvEC*_032) were most

13643703, 2026, 9, Downloaded from https://bsppjournals.onlinelibrary.wiley.com/doi/10.1111/mpp.70341 by Cochrane Colombia, Wiley Online Library on [12/11/2026]. See the Terms and Conditions (https://onlinelibrary.wiley.com/terms-and-conditions) on Wiley Online Library for rules of use; OA articles are governed by the applicable Creative Commons License

highly expressed during the pre-biotrophic phase. *HvEC*_036 and *HvEC*_040 reached peak transcript abundance in dormant urediniospores, whereas *HvEC*_028 and *HvEC*_032 peaked during urediniospore germination (Figure 4a,b). Although predominantly associated with early development, these genes remained expressed during the initial stages of host colonization,

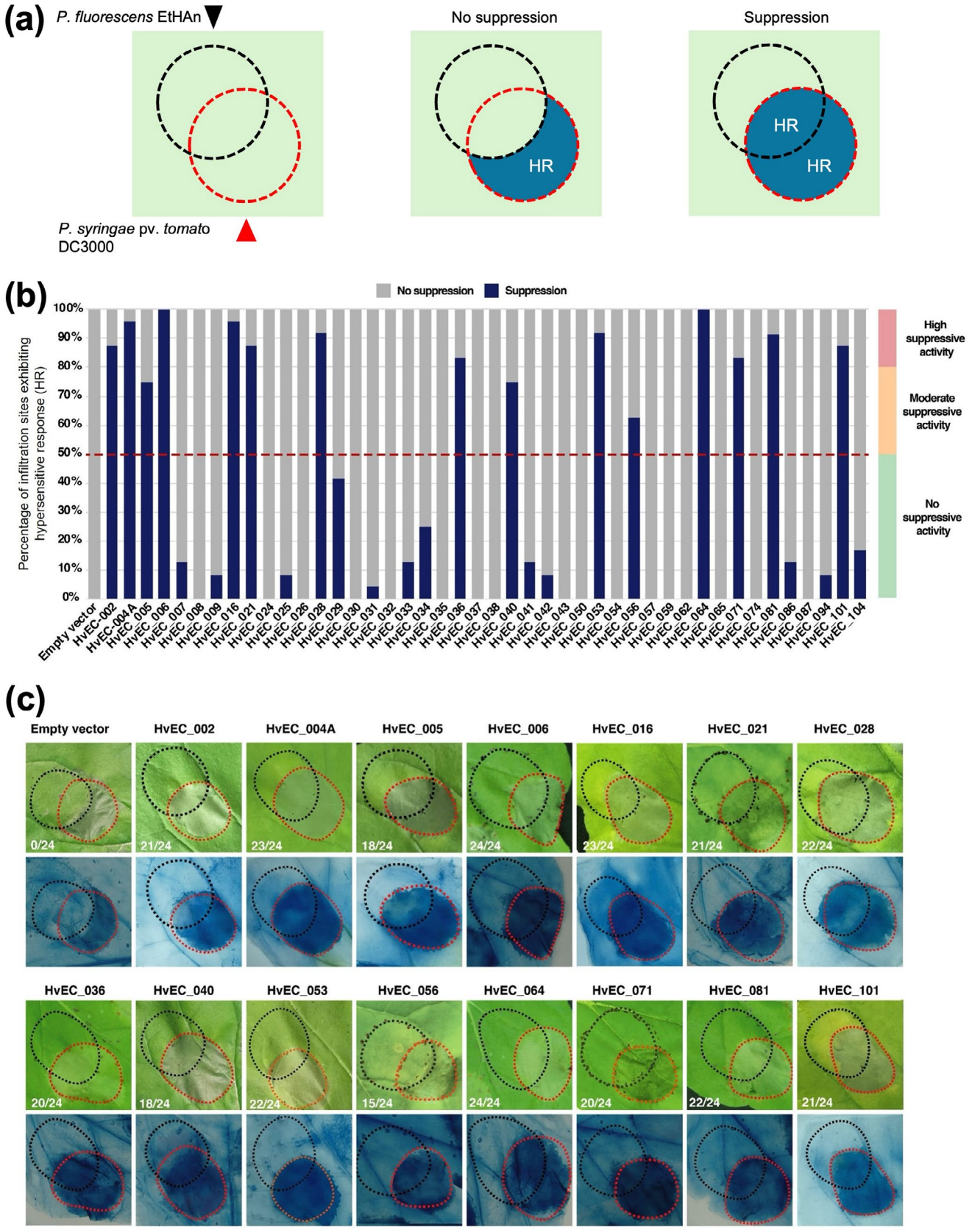


FIGURE 1 | Legend on next page.

13643703, 2026, 9, Downloaded from https://bsppjournals.onlinelibrary.wiley.com/doi/10.1111/mpp.70341 by Cochrane Colombia, Wiley Online Library on [12/11/2026]. See the Terms and Conditions (https://onlinelibrary.wiley.com/terms-and-conditions) on Wiley Online Library for rules of use; OA articles are governed by the applicable Creative Commons License

FIGURE 1 | Pattern-triggered immunity (PTI) suppression by *Hemileia vastatrix* effector candidates (HvECs) in *Nicotiana benthamiana*. (a) Schematic representation of the PTI suppression assay. Left, a *N. benthamiana* leaf was infiltrated with the nonpathogenic *Pseudomonas fluorescens* EtHAn (black dashed circle), followed 7 h later by infiltration with the pathogenic *Pseudomonas syringae* pv. *tomato* DC3000 (red dashed circle) into an overlapping region. Middle, in the absence of a PTI-suppressing effector, PTI elicited by *P. fluorescens* EtHAn restricts subsequent *P. syringae* pv. *tomato* DC3000 growth, preventing the bacterial population from reaching the level required to deliver sufficient Type III effectors to trigger a visible hypersensitive response (HR) in the overlapping region ('No suppression'). Right, delivery of a PTI-suppressing HvEC by *P. fluorescens* EtHAn attenuates this immune response, allowing greater subsequent growth of *P. syringae* pv. *tomato* DC3000 and sufficient Type III effector delivery to trigger visible HR throughout the overlapping region ('Suppression'). (b) PTI suppression assay using the *P. fluorescens* EtHAn-adapted EDV system performed with 44 HvECs (pEDV6::*HvEC* constructs) and an empty vector control. PTI suppression was quantified as the percentage of infiltration sites displaying HR relative to the total number of infiltrated sites (three independent experiments, each comprising eight biological replicates; total $n = 24$). HR was scored specifically in the overlapping region between the two bacterial infiltrations. Candidate effectors that restored *P. syringae* pv. *tomato* DC3000-induced HR in ≥ 50% of infiltration sites were classified as PTI suppressors. The red dashed line indicates this classification threshold. (c) Representative macroscopic photographs showing the phenotypic outcomes of the PTI suppression assay. Suspensions of *P. fluorescens* EtHAn expressing pEDV6::*HvEC* constructs or empty vector (2×10^7 CFU mL^{-1}) were infiltrated into the abaxial side of *N. benthamiana* leaves (black dashed circle). Seven hours later, *P. syringae* pv. *tomato* DC3000 (3×10^6 CFU mL^{-1}) was infiltrated into an overlapping region (red dashed circle). Images were taken 72 h after DC3000 infiltration. Lower panels show trypan blue staining to visualize dead cells. Values indicate the number of infiltration sites showing HR out of the total number evaluated ($n = 24$). Restoration of HR in the overlapping region indicates suppression of PTI by the corresponding HvEC.

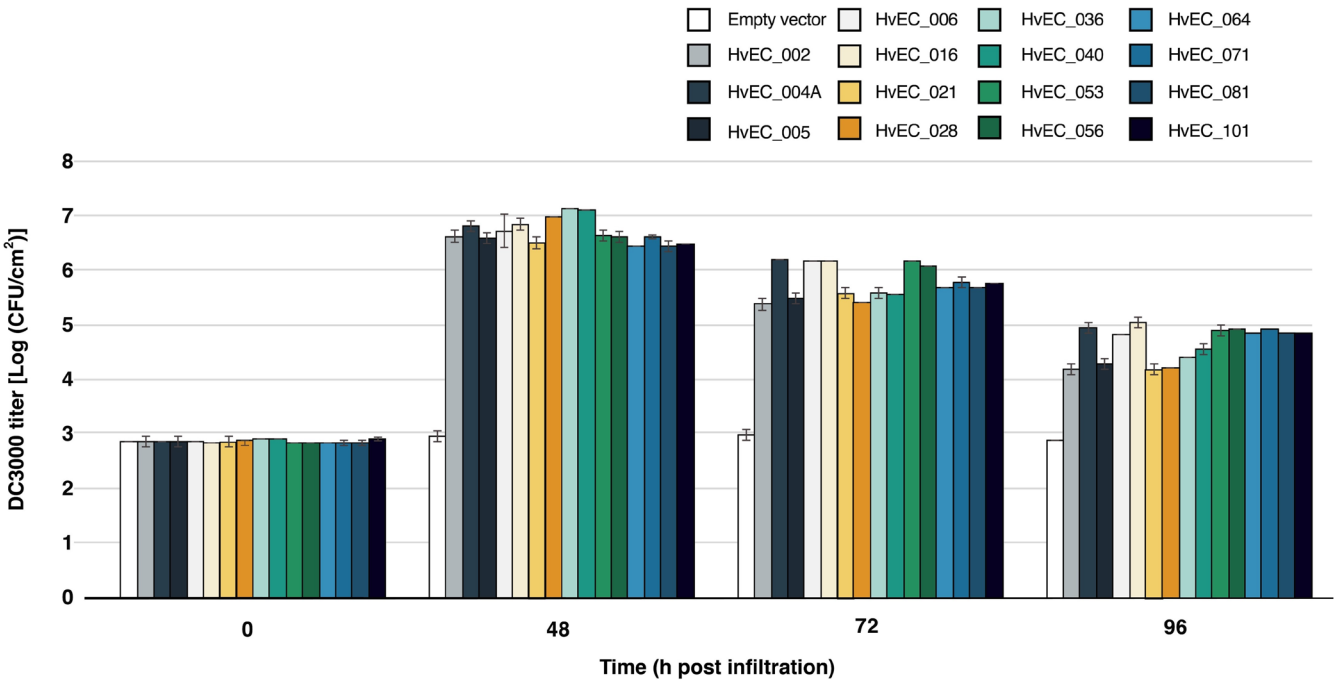


FIGURE 2 | *Hemileia vastatrix* effector candidates (HvECs) promote *Pseudomonas syringae* pv. *tomato* DC3000 growth in *Nicotiana benthamiana*. Bacterial suspensions of *Pseudomonas fluorescens* EtHAn carrying the empty pEDV6 vector or expressing individual pEDV6::*HvEC* constructs (5×10^6 CFU mL^{-1}) were pre-infiltrated into *N. benthamiana* leaves. Seven hours later, a suspension of *P. syringae* pv. *tomato* DC3000 (1×10^5 CFU mL^{-1}) was infiltrated into an overlapping region. Bacterial populations of DC3000 were quantified as colony-forming units (CFU) from 1-cm-diameter leaf disks collected at 0, 48, 72 and 96 h after infiltration. Leaf disks were macerated, serially diluted and plated on King's B medium containing rifampicin (100 μg mL^{-1}). Bars represent the mean ± SE of three independent biological replicates.

with *HvEC*_032 maintaining detectable transcript levels throughout the biotrophic phase.

A second group of *HvEC*s exhibited maximum expression after host penetration. *HvEC*_004A and *HvEC*_005 were strongly induced at 24 h post-inoculation (hpi), coinciding with fungal penetration and the establishment of biotrophy (Figure 4c). *HvEC*_004A remained highly expressed throughout the subsequent infection stages, whereas *HvEC*_005 exhibited a pronounced but transient induction during penetration.

In contrast, *HvEC*_002 accumulated predominantly during the later stages of colonization, reaching its highest transcript levels at 9 and 15 days post-inoculation (dpi) (Figure 4d), suggesting a role in maintaining the biotrophic interaction.

Overall, the temporal expression profiles indicate that HvECs are deployed sequentially throughout infection, from urediniospore germination to late biotrophic colonization, supporting the hypothesis that distinct subsets of effectors contribute to successive stages of host manipulation during infection.

13643703, 2026, 9, Downloaded from https://bsppjournals.onlinelibrary.wiley.com/doi/10.1111/mpp.70341 by Cochrane Colombia, Wiley Online Library on [12/11/2026]. See the Terms and Conditions (https://onlinelibrary.wiley.com/terms-and-conditions) on Wiley Online Library for rules of use; OA articles are governed by the applicable Creative Commons License

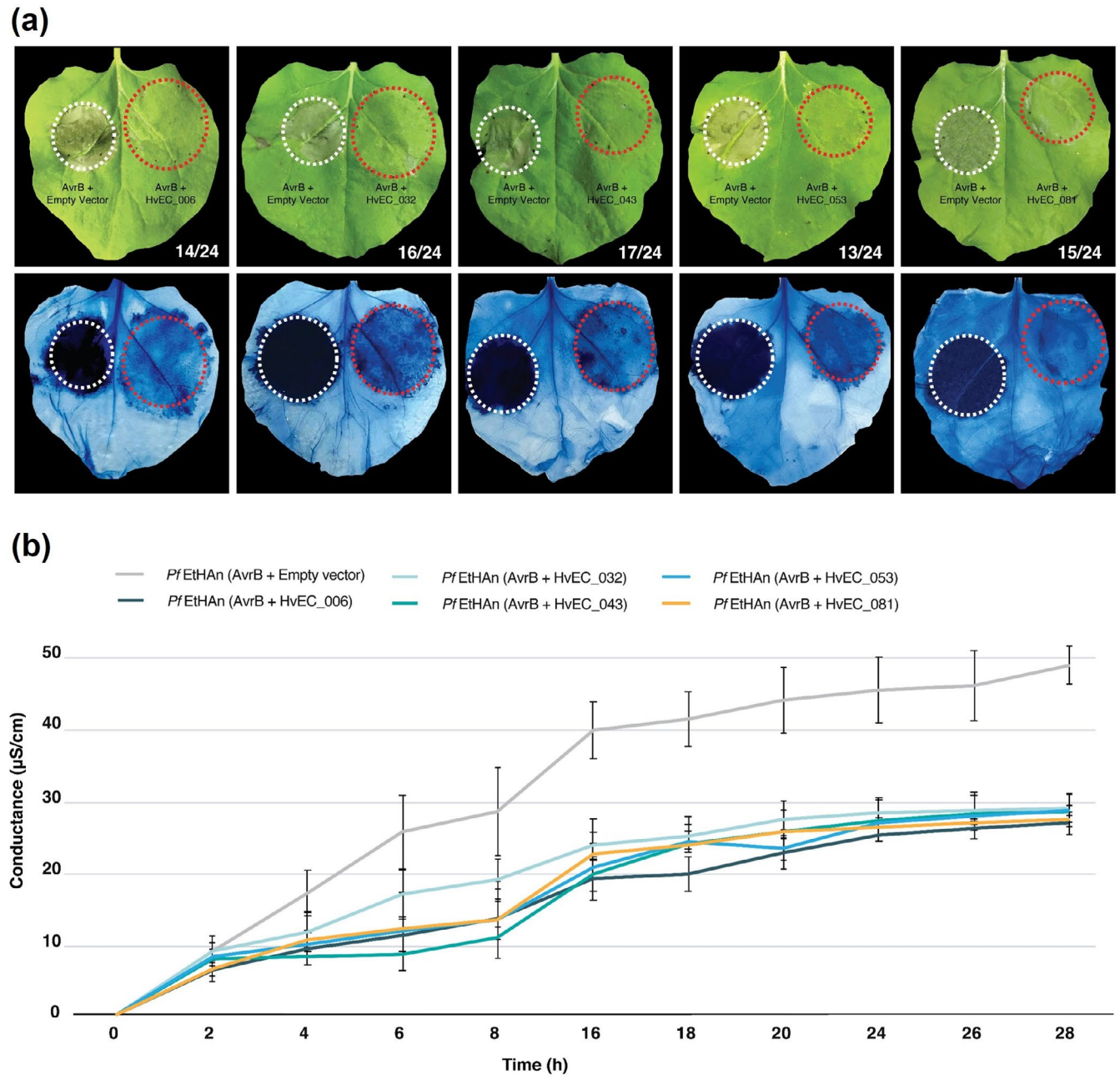


FIGURE 3 | Suppression of AvrB-induced effector-triggered immunity (ETI) by *Hemileia vastatrix* effector candidates (HvECs) in *Nicotiana benthamiana*. (a) *N. benthamiana* leaves showing suppression of AvrB-induced hypersensitivity response (HR) by five HvECs (HvEC_006, HvEC_032, HvEC_043, HvEC_053 and HvEC_081). Bacterial suspensions of *Pseudomonas fluorescens* EtHAn expressing p*VSP6*::*AvrB* and *P. fluorescens* EtHAn expressing the empty pEDV6 vector were mixed (1:1 ratio) to a final concentration of 2×10^7 CFU mL^{-1} and used as controls (white dashed circle). Suspensions of *P. fluorescens* EtHAn expressing p*VSP6*::*AvrB* and *P. fluorescens* EtHAn expressing individual pEDV6::*HvEC* constructs were co-infiltrated under the same conditions (red dashed circle). Images were taken 48 h after infiltration. ETI suppression was quantified as the percentage of infiltration sites in which AvrB-induced HR was reduced or absent, relative to the total number of infiltrated sites (three independent experiments, each comprising eight biological replicates; total $n = 24$). Lower panels show trypan blue staining to visualize dead cells. (b) Electrolyte leakage assay to quantify AvrB-induced cell death. Leaf disks (8 mm diameter) from *N. benthamiana* were collected after co-infiltration and incubated in 5 mL of sterile deionized water. Conductivity (µS cm^{-1}) was measured over a 0–28 h period and plotted as a function of time. Values represent the mean ± SE of four independent biological replicates.

2.4 | HvECs Target Distinct Plant Subcellular Compartments

To gain insight into their potential modes of action, the subcellular localization of 11 HvEC-GFP fusion proteins was examined by transient expression in *N. benthamiana* leaves.

Nine HvECs accumulated in defined cellular compartments (Figures 5 and 6). Six proteins localized predominantly to the nucleus. HvRTP_01B-GFP, HvEC_004A-GFP and HvEC_040-GFP accumulated mainly in the nucleus while retaining weak cytoplasmic fluorescence, indicating nucleocytoplasmic localization (Figure 5a). In contrast, HvEC_006-GFP,

13643703, 2026, 9, Downloaded from https://bsppjournals.onlinelibrary.wiley.com/doi/10.1111/mpp.70341 by Cochrane Colombia, Wiley Online Library on [12/11/2026]. See the Terms and Conditions (https://onlinelibrary.wiley.com/terms-and-conditions) on Wiley Online Library for rules of use; OA articles are governed by the applicable Creative Commons License

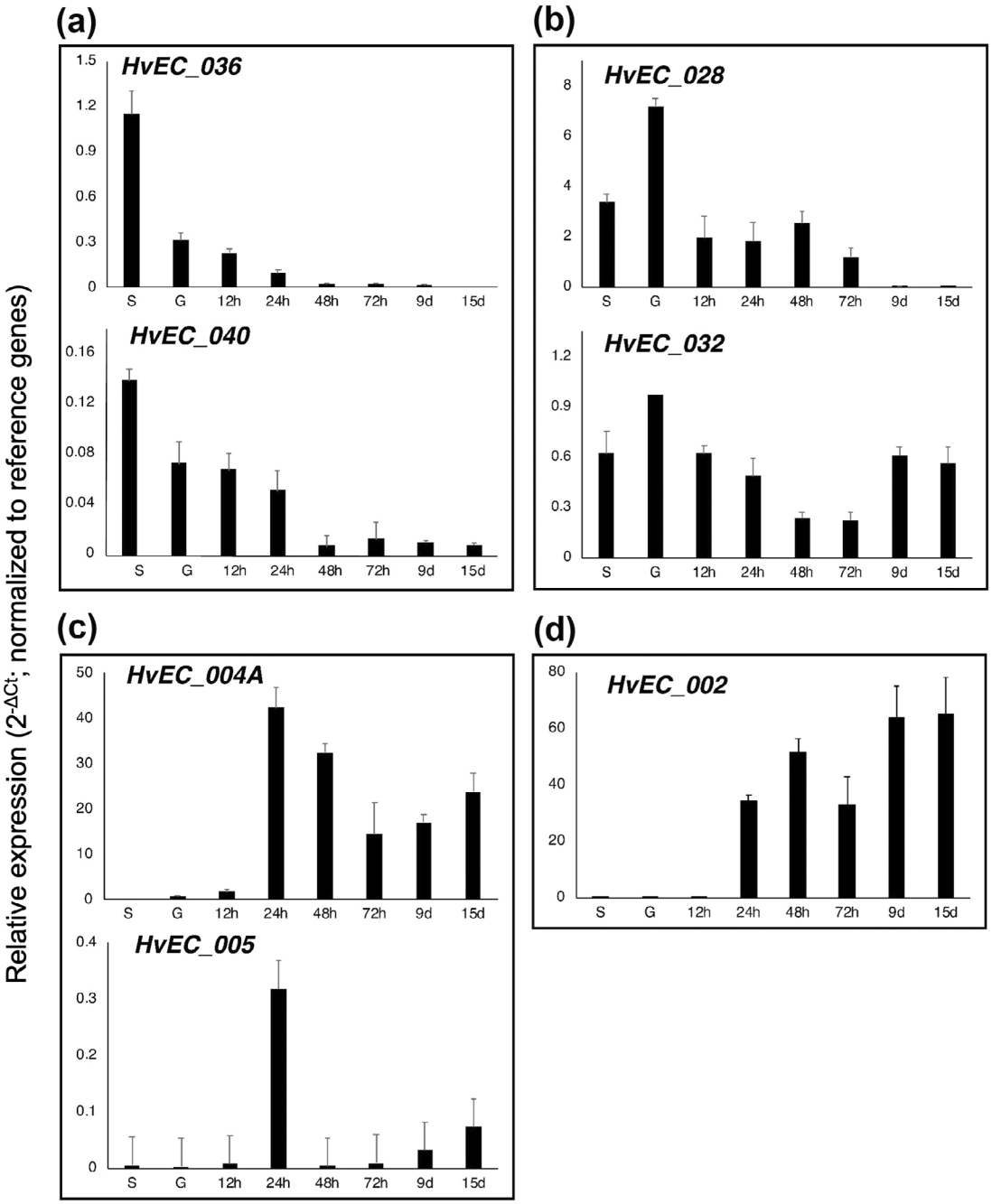


FIGURE 4 | Expression profiling of seven *HvEC* genes associated with suppression of plant immunity. Transcript accumulation was quantified by reverse transcription-quantitative PCR (RT-qPCR) in samples obtained from dormant urediniospores (U), urediniospores germinated on polystyrene plates (G) and infected coffee leaves collected at 12, 24, 48 and 72 h post-inoculation (hpi), and 9 and 15 days post-inoculation (dpi). (a) *HvEC_036* and *HvEC_040* with highest peaks in dormant urediniospores. (b) *HvEC_028* and *HvEC_032* showing highest expression in germinated urediniospores. (c) *HvEC-004A* and *HvEC-005* with highest peaks at 24 hpi. (d) *HvEC-002* with highest peaks at 9 and 15 dpi. Bars represent the mean ± SE of relative transcript abundance ($2^{-\Delta C_t}$) from three independent biological replicates. ΔC_t values were calculated using mean C_t values of three endogenous reference *H. vastatrix* genes (*Cytochrome c oxidase subunit III*, *Glyceraldehyde-3-phosphate dehydrogenase* and *β-tubulin*). For each biological replicate, qPCRs were performed in technical duplicate, and the C_t values were averaged before analysis.

HvEC_016-GFP and HvEC_036-GFP were concentrated in the nucleoplasm, with no obvious accumulation in the nucleolar region (Figure 5b). Nuclear localization was confirmed by co-localization with the *Arabidopsis thaliana* nucleoplasmic marker AtWWP1-mCherry (Silva et al. 2015); as this marker labels the nucleoplasm rather than the nucleolus specifically, definitive confirmation of nucleolar exclusion would require co-localization with a dedicated nucleolar marker such as fibrillarin (Zheng et al. 2016).

Three HvECs (HvEC_021-GFP, HvEC_053-GFP and HvEC_056-GFP) localized exclusively to chloroplasts (Figure 6). Conversely, HvEC_028-GFP and HvEC_101-GFP displayed diffuse fluorescence without obvious compartment specificity (Figure S2),

13643703, 2026, 9, Downloaded from https://bsppjournals.onlinelibrary.wiley.com/doi/10.1111/mpp.70341 by Cochrane Colombia, Wiley Online Library on [12/11/2026]. See the Terms and Conditions (https://onlinelibrary.wiley.com/terms-and-conditions) on Wiley Online Library for rules of use; OA articles are governed by the applicable Creative Commons License

TABLE 1 | Seventeen *Hemileia vastatrix* effector candidates (HvECs) conferring plant immune suppression activity.

HvECs[a]	Length[b]	No. of Cys[c]	cDNA library[d]	Suppression activity[e]		Gene expression[f,g]
				PTI	ETI	
HvEC_002	77	0	Biotrophic growth	Yes	No	I
HvEC_004A	173	2	Biotrophic growth	Yes	No	P
HvEC_005	172	9	Biotrophic growth	Yes	No	P
HvEC_006	111	0	Biotrophic growth	Yes	Yes	I
HvEC_016	201	7	Biotrophic growth	Yes	No	I
HvEC_021	174	12	Biotrophic growth	Yes	No	I
HvEC_028	267	0	Spore germination	Yes	No	G
HvEC_032	62	1	Spore germination	No	Yes	G
HvEC_036	75	0	Spore germination	Yes	No	S
HvEC_040	84	1	Spore germination	Yes	No	S
HvEC_043	52	0	Spore germination	No	Yes	I
HvEC_053	113	0	Biotrophic growth	Yes	Yes	P, I
HvEC_056	268	9	Biotrophic growth	Yes	No	I
HvEC_064	106	10	Biotrophic growth	Yes	No	S, G, I
HvEC_071	91	6	Biotrophic growth	Yes	No	P, I
HvEC_081	100	6	Biotrophic growth	Yes	Yes	I
HvEC_101	83	2	Biotrophic growth	Yes	No	I

[a]Candidate effectors predicted from cDNA libraries constructed from different stages of *H. vastatrix* lifecycle (Maia, Badel, Marin-Ramirez, et al. 2017).
[b]Number of amino acids indicated in the mature form of the protein (i.e., without the signal peptide).
[c]Number of cysteine residues in the mature form of the protein.
[d]Stages of infection used for cDNA library constructions to identify these effector candidates (Maia, Badel, Marin-Ramirez, et al. 2017).
[e]Data of plant immunity suppression assays using EtHAn-adapted EDV system in *Nicotiana benthamiana* from this study.
[f]Highest transcript accumulation: S = dormant spores, G = germlings, P = penetration (12–24 hpi), I = infected leaves (after 48 hpi).
[g]Data from both this and our previous studies (Maia, Badel, Marin-Ramirez, et al. 2017).

whereas free GFP was distributed uniformly throughout the cytoplasm and nucleus (Figure S3).

3 | Discussion

Suppression of host immunity is one of the best-characterized activities of filamentous pathogen effectors and a common prerequisite for successful colonization of living host tissues (Rocafort et al. 2020; Ngou, Ding, and Jones 2022; Li et al. 2024). Accordingly, effector biology has evolved from identifying candidate secreted proteins towards understanding how entire repertoires manipulate interconnected immune networks throughout infection (Li et al. 2024; Petre et al. 2014; Henningsen et al. 2025). Consistent with this perspective, 15 of the 44 HvECs examined consistently suppressed PTI when delivered into *N. benthamiana* using the *P. fluorescens* EtHAn Type III secretion system. Their ability to restore tissue viability following Pf EtHAn infiltration while simultaneously promoting increased proliferation of Pto DC3000 demonstrates that these proteins actively interfere with conserved immune processes rather than simply delaying host cell death. Similar results have been reported for effectors from diverse filamentous pathogens using the same experimental platform (Badel et al. 2013; Cheng et al. 2017; Ramachandran et al. 2017; Qi et al. 2019; Maia et al. 2022), reinforcing the utility of this heterologous system for functional characterization when studies in the native host remain experimentally inaccessible.

Approximately one-third of the HvECs reproducibly suppressed PTI, indicating that immune suppression is a common property of the *H. vastatrix* secretome rather than a feature restricted to a few specialized proteins. Comparable proportions have been reported in other rust fungi and biotrophic pathogens, where only subsets of predicted secreted proteins exhibit measurable immune-suppressive activity despite widespread transcription during infection (Petre et al. 2014; Rocafort et al. 2020). This apparent functional specialization likely reflects the evolutionary diversification of effector repertoires, in which individual proteins fulfill complementary roles during successive stages of infection. The relatively high frequency of PTI suppressors identified here therefore supports the view that successful colonization depends on multiple effectors targeting distinct components of the coffee immune system, not on a single effector.

13643703, 2026, 9, Downloaded from https://bsppjournals.onlinelibrary.wiley.com/doi/10.1111/mpp.70341 by Cochrane Colombia, Wiley Online Library on [12/11/2026]. See the Terms and Conditions (https://onlinelibrary.wiley.com/terms-and-conditions) on Wiley Online Library for rules of use; OA articles are governed by the applicable Creative Commons License

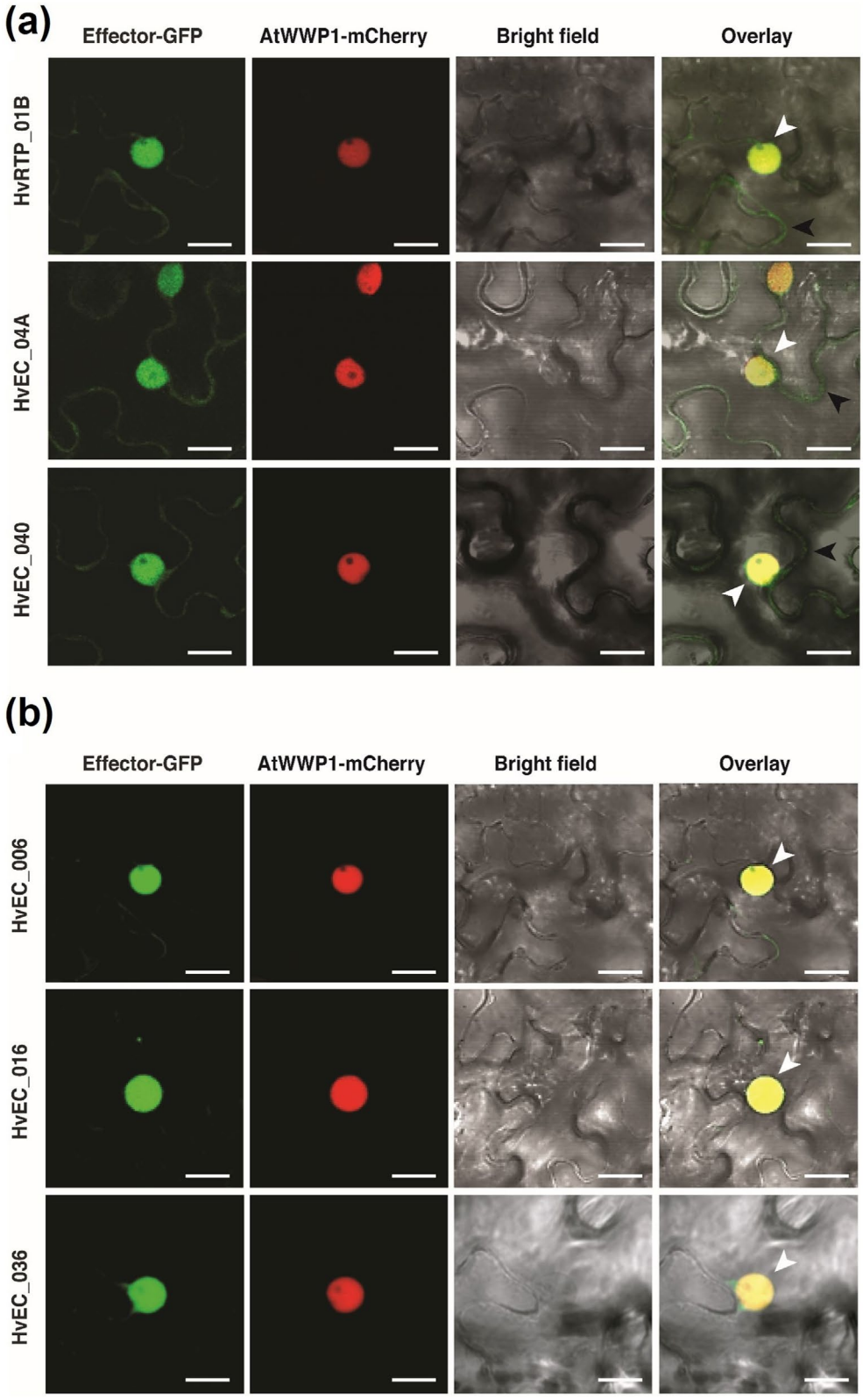


FIGURE 5 | Subcellular localization of C-terminally GFP-tagged *Hemileia vastatrix* effector candidate fusions (HvECs-GFP) in plant nuclei. (a) Nucleocytoplasmatic localization of three fusion proteins HvRTP_01B-GFP, HvEC_004A-GFP and HvEC_040-GFP. (b) Specific nuclear localization of three fusion proteins HvEC_006-GFP, HvEC_016-GFP and HvEC_036-GFP. Bacterial suspensions of *Agrobacterium tumefaciens* GV3101 (pMP90) carrying *HvEC-GFP* fusion constructs and same strain carrying the nuclear marker AtWWP1-mCherry (Silva et al. 2015) fusion construct were co-infiltrated (1:1 ratio) to a final of 4×10^7 CFU mL^{-1} into *Nicotiana benthamiana* leaves. About 72 h after co-infiltrations, leaf disks were sampled and viewed by confocal microscopy. GFP and mCherry were excited at 488 and 561 nm, respectively. GFP (green) and mCherry (red) fluorescence were collected at 505–525 and 580–620 nm, respectively. Scale bars = 20 μm.

13643703, 2026, 9, Downloaded from https://bsppjournals.onlinelibrary.wiley.com/doi/10.1111/mpp.70341 by Cochrane Colombia, Wiley Online Library on [12/11/2026]. See the Terms and Conditions (https://onlinelibrary.wiley.com/terms-and-conditions) on Wiley Online Library for rules of use; OA articles are governed by the applicable Creative Commons License

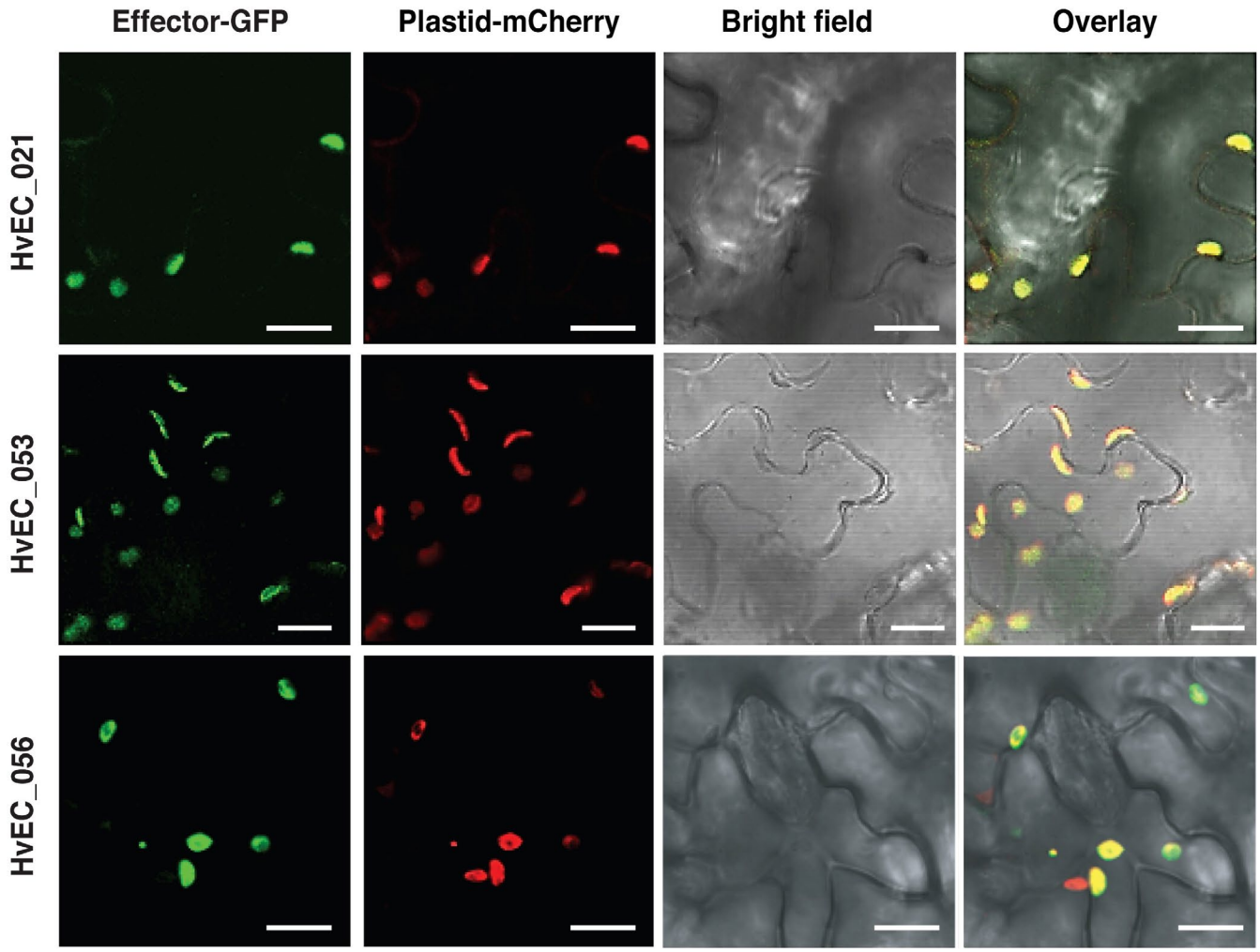


FIGURE 6 | Subcellular localization of C-terminally GFP-tagged *Hemileia vastatrix* effector candidate fusions (HvECs-GFP) in chloroplasts. Three fusion proteins, HvEC_021-GFP, HvEC_053-GFP and HvEC_056-GFP, are localized to chloroplast compartments when transiently expressed in *Nicotiana benthamiana* leaf cells. Bacterial suspensions of *Agrobacterium tumefaciens* GV3101 (pMP90) carrying *HvEC-GFP* fusion constructs and the same strain carrying the small subunit of tobacco RuBisCO-mCherry fusion construct (plastid marker) were co-infiltrated (1:1 ratio) to a final concentration of 4×10^7 CFU mL^{-1} into *N. benthamiana* leaf cells. About 72 h post-agroinfiltrations, leaf disks were sampled and viewed by confocal microscopy. GFP and mCherry were excited at 488 and 561 nm, respectively. GFP (green) and mCherry (red) were collected at 505–525 and 580–620 nm, respectively. Scale bars = 20 μm.

Current models of plant immunity recognize PTI and ETI as highly interconnected signalling networks rather than independent defence layers (Yuan et al. 2021; Ngou, Ding, and Jones 2022). Activation of intracellular NLR receptors amplifies PTI outputs, whereas PTI provides essential components required for full ETI activation, creating extensive molecular crosstalk between these immune pathways. Consequently, effectors capable of attenuating both PTI and ETI are expected to interfere with conserved regulatory nodes positioned upstream of immune network divergence. In agreement with this model, five HvECs attenuated AvrB-triggered ETI, three of which (HvEC_006, HvEC_053 and HvEC_081) also suppressed PTI. This dual suppressive capacity does not appear to reflect unrelated activities but instead suggests that these HvECs target central regulators shared by both immune pathways.

Although the molecular targets of HvECs remain unknown, studies in bacterial and fungal pathogens provide plausible mechanistic hypotheses. Diverse effectors converge on conserved immune hubs, including receptor-like cytoplasmic kinases, RIN4-associated complexes, MAP kinase cascades, vesicle trafficking machinery and ubiquitin-mediated protein turnover, thereby simultaneously attenuating PTI- and ETI-associated responses (Feng et al. 2012; Xu et al. 2017; Redditt et al. 2019; Ngou, Ding, and Jones 2022). Likewise, fungal effectors frequently manipulate central regulatory nodes rather than pathway-specific components, enabling relatively few proteins to exert broad effects on plant immunity (Rocafort et al. 2020). Whether HvEC_006, HvEC_053 and HvEC_081 converge on similar host targets remains to be determined, but their dual suppressive activity identifies them as particularly strong candidates for future studies aimed at elucidating their molecular functions and interacting host proteins.

Although these experiments were performed in a heterologous system, several lines of evidence support their biological relevance. Core immune signalling pathways are remarkably conserved across dicot species, and homologues of both RIN4

13643703, 2026, 9, Downloaded from https://bsppjournals.onlinelibrary.wiley.com/doi/10.1111/mpp.70341 by Cochrane Colombia, Wiley Online Library on [12/11/2026]. See the Terms and Conditions (https://onlinelibrary.wiley.com/terms-and-conditions) on Wiley Online Library for rules of use; OA articles are governed by the applicable Creative Commons License

(GenBank accession XP_027114570.2) and RIPK (GenBank accession XP_071908951.1) were identified in *Coffea arabica*, including strong conservation of their kinase domains. It should be noted, however, that sequence conservation of RIN4 and RIPK does not by itself demonstrate that the AvrB-RPM1-RIN4 signalling module operates identically in coffee; functional validation of this pathway in *C. arabica* remains an important direction for future work. Similar conservation has been demonstrated for several PTI- and ETI-associated signalling components across angiosperms (Ngou, Heal, et al. 2022), explaining why *N. benthamiana* has become an effective platform for functional analyses of effectors from phylogenetically diverse pathogens. While individual molecular interactions will ultimately require validation in coffee, the convergence of immune-suppression assays with conserved immune signalling, temporal expression and subcellular localization provide strong evidence that the HvECs identified here represent biologically relevant components of the *H. vastatrix* infection repertoire.

The prolonged biotrophic lifestyle of *H. vastatrix* provides an important biological context for interpreting these findings. Following penetration through stomata, the fungus establishes haustoria and maintains intimate interactions with living host cells for nearly 4 weeks before sporulation begins (Silva et al. 1999; Maia, Badel, Fernandes, et al. 2017). Sustaining compatibility with living host tissues over such an extended period is unlikely to depend on the constitutive activity of a few individual effectors. Instead, these results support the view that *H. vastatrix* relies on successive cohorts of functionally specialized effectors that collectively maintain immune suppression throughout infection, thereby promoting fungal pathogenesis and long-term biotrophic colonization.

This functional specialization is further supported by the temporal regulation of HvEC expression during infection. Increasing evidence from filamentous pathogens indicates that the biological significance of an effector may depend not only on its molecular activity but also on the stage of infection at which it is expressed and delivered (Rocafort et al. 2020; Petre et al. 2014). Integrating temporal expression with functional characterization therefore provides biological context that cannot be inferred from transcriptomic or immune-suppression analyses alone.

The temporal expression profiles obtained here, together with those previously reported by Maia, Badel, Marin-Ramirez, et al. (2017), indicate that *H. vastatrix* deploys successive waves of effectors throughout infection. Seven candidate effector genes (*HvEC*_004A, *HvEC*_005, *HvEC*_054, *HvEC*_059, *HvEC*_071, *HvEC*_084 and *HvEC*_125) reached peak transcript accumulation at 24 hpi, coinciding with fungal penetration and the earliest stages of host colonization. During this period, germ tubes differentiate substomatal vesicles, primary hyphae and haustorial mother cells before establishing the first haustoria within subsidiary and mesophyll cells (Silva et al. 1999). These developmental transitions expose the pathogen to intense immune surveillance, making early suppression of host defences particularly important for successful establishment. The coordinated induction of these *HvECs* therefore strongly suggests that their encoded proteins contribute to overcoming the first immune barriers encountered immediately after penetration.

Interestingly, four PTI-suppressing effectors (HvEC_028, HvEC_032, HvEC_036 and HvEC_040) exhibited maximum transcript accumulation in dormant or germinated urediniospores, prior to appressorium formation and stomatal penetration. These candidates were originally identified from the HEVA-Sanger cDNA library generated from germinated urediniospores (Maia, Badel, Marin-Ramirez, et al. 2017), but their biological significance remained unresolved. Their functional characterization demonstrates that these proteins actively suppress plant immunity. This finding is consistent with, and extends, growing evidence that molecules relevant to the plant–rust fungi interactions can act at the spore or germling stage, well before host penetration or haustorium formation. In the barley–*Puccinia graminis* f. sp. *tritici* system, host recognition of urediniospore-associated proteins occurs within minutes of spore contact, and virulence-associated proteins have been isolated directly from ungerminated spores, both acting long before haustorium formation (Nirmala et al. 2010, 2011). Similarly, a virulence-contributing effector protein was recently identified in germinated urediniospores of *Puccinia triticina* (Ozketen et al. 2026). Our results corroborate this emerging pre-penetration paradigm in *H. vastatrix* and suggest that immune modulation may begin as early as spore adhesion to the host leaf surface, prior to stomatal penetration and haustorium formation. Consequently, studies focused exclusively on *in planta* transcript accumulation are likely to underestimate the contribution of pre-penetration effectors to fungal pathogenesis.

Temporal coordination of effector deployment has emerged as a common feature of filamentous pathogens. In rust fungi, transcriptomic studies consistently associate distinct subsets of secreted proteins with successive developmental stages, including spore germination, penetration, haustorium differentiation and maintenance of biotrophy (Petre et al. 2014; Rocafort et al. 2020). Similar patterns have been described in both biotrophic and hemibiotrophic pathogens, where successive waves of effectors facilitate transitions between infection stages rather than functioning as constitutively expressed proteins (Kleemann et al. 2012; Lorrain et al. 2019). Our results extend this concept by demonstrating that temporally regulated HvECs include proteins with experimentally validated immune-suppressive activity, providing functional evidence that these transcriptional programmes reflect biologically meaningful transitions during *H. vastatrix* pathogenesis rather than simple developmental changes.

The unusually long latent period of coffee leaf rust further emphasizes the importance of this regulatory strategy. Unlike rapidly necrotizing pathogens, *H. vastatrix* must maintain host cell viability for several weeks while continuously acquiring nutrients through haustoria. As infection progresses, the physiological status of the host and the intensity of immune responses inevitably change, making it unlikely that a single constitutively expressed set of effectors would remain equally effective throughout colonization. Sequential deployment of functionally specialized effectors therefore provides a flexible strategy by which the fungus can continuously adjust host manipulation while maintaining compatibility with living tissues. Such temporal regulation may also reduce selective pressure acting on individual effectors, thereby contributing to the long-term

13643703, 2026, 9, Downloaded from https://bsppjournals.onlinelibrary.wiley.com/doi/10.1111/mpp.70341 by Cochrane Colombia, Wiley Online Library on [12/11/2026]. See the Terms and Conditions (https://onlinelibrary.wiley.com/terms-and-conditions) on Wiley Online Library for rules of use; OA articles are governed by the applicable Creative Commons License

maintenance of compatible interactions despite the continuous evolution of host immune systems.

Temporal expression alone, however, does not fully explain effector function. Successful host manipulation also depends on the intracellular destination of these proteins after delivery into host cells. Increasing evidence indicates that pathogen effectors preferentially target intracellular compartments functioning as regulatory hubs rather than being randomly distributed throughout the host cell (Petre et al. 2016; Figueroa et al. 2021). In this context, defining the subcellular destinations of HvECs provides mechanistic insight into the host cellular processes targeted during infection.

Six HvEC–GFP fusion proteins accumulated predominantly within the nucleoplasm, with no obvious nucleolar accumulation, tentatively suggesting that these effectors may target processes associated with transcriptional regulation rather than ribosome biogenesis; confirming this would require colocalization with a dedicated nucleolar marker, as only a nucleoplasmic marker was used here. The nucleus has emerged as one of the principal destinations of filamentous pathogen effectors because it integrates transcriptional reprogramming, chromatin remodelling, RNA processing, hormone signalling and NLR-mediated immune responses (Petre et al. 2016; Rocafort et al. 2020). Numerous rust fungal effectors exploit these regulatory processes. For example, the *Melampsora larici-populina* effector Mlp124478 functions as a DNA-binding protein that suppresses defence-associated transcription (Ahmed et al. 2018), whereas the *Phakopsora pachyrhizi* effector PpEC23 interacts with the soybean transcription factor GmSP12I to attenuate both host and non-host immunity (Qi et al. 2016). Likewise, members of the Rust Transferred Protein (RTP) family accumulate within host nuclei following translocation from fungal haustoria (Kemen et al. 2005; Qi et al. 2019). The predominance of nucleoplasmic localization observed here therefore suggests that *H. vastatrix* similarly manipulates nuclear regulatory networks, reinforcing the importance of transcriptional reprogramming during rust fungal pathogenesis.

Three HvECs localized specifically to chloroplasts, extending previous observations that plastids are major targets of pathogen effectors across bacteria, fungi, oomycetes and viruses (Nomura et al. 2012; Sowden et al. 2018). Beyond photosynthesis, chloroplasts coordinate multiple defence-associated processes, including reactive oxygen species (ROS) production, calcium signalling, salicylic acid biosynthesis, jasmonate metabolism and retrograde signalling to the nucleus, making them central regulators of plant immunity. These subcellular localization patterns, both nuclear and chloroplastic, were obtained under constitutive CaMV 35S-driven overexpression in *N. benthamiana*, a non-host species for *H. vastatrix* used here solely as a transient expression system, and may not fully recapitulate native HvEC expression levels, host-specific interactions or subcellular dynamics during infection of coffee, the natural host.

Evidence from other rust fungi further highlights the importance of chloroplast-targeted effectors during infection. The *M. larici-populina* effector CTP1 belongs to a conserved family of plastid-targeted proteins within the Melampsoraceae (Petre et al. 2016). In *P. striiformis* f. sp. *tritici*, Pst_12806 suppresses chloroplast-associated immunity through interaction with TaISP, a component of the cytochrome b_6f complex (Xu et al. 2019), whereas Pst11215 targets host mitochondria to interfere with immune activation (Pan et al. 2025). More recently, Pst_TTP1 was shown to inhibit chloroplast import of the thioredoxin TaTrx, thereby suppressing ROS accumulation, delaying senescence and promoting prolonged biotrophy (Li et al. 2025). Collectively, these studies indicate that rust fungi preferentially manipulate intracellular organelles that integrate immune signalling rather than isolated defence components. The chloroplast localization of HvEC_021, HvEC_053 and HvEC_056 therefore identifies plastid-associated immune regulation as a likely target of *H. vastatrix* during coffee infection.

An important implication of this work is its contribution to identifying candidate avirulence determinants involved in *SH*-mediated resistance. Although HvEC-016 remains the only experimentally validated avirulence effector that may be recognized by an *SH* resistance protein (Maia, Badel, Marin-Ramirez, et al. 2017), the present study identifies several HvECs that combine biological characteristics expected for proteins involved in host immune recognition. Effectors that suppress plant immunity, are expressed at biologically appropriate stages of infection and accumulate within immune regulatory compartments constitute particularly strong candidates for future studies aimed at elucidating the molecular basis of *SH*-mediated resistance.

Functional validation of these candidates will require complementary approaches, including interaction studies with coffee proteins, transient expression assays in coffee tissues, structural prediction, protein–protein interaction analyses and reverse-genetic strategies. Until stable transformation or reverse-genetic tools become available for *H. vastatrix*, transient delivery of candidate HvECs using the Pf EtHAn system provides a practical platform for accelerating *Avr* gene discovery. Combined with genetic cosegregation analyses in coffee populations segregating for specific *SH* resistance genes, this experimental platform would enable direct evaluation of candidate effectors for *SH*-specific immune recognition.

When considered together, the functional, temporal and localization datasets reveal a coherent pattern of effector deployment during infection. Immune-suppressive activity identifies proteins capable of modulating host defences, temporal expression defines the developmental stages at which these activities are required, and subcellular localization indicates the host compartments where they are most likely to operate. Rather than acting as independent proteins with isolated functions, HvECs appear to constitute a coordinated repertoire deployed sequentially throughout infection to manipulate complementary components of the host immune system. This integrated view moves beyond descriptive cataloguing of candidate effectors and provides a biologically grounded model for understanding how *H. vastatrix* sustains prolonged biotrophic colonization, while establishing a foundation for elucidating the molecular basis of *SH*-mediated resistance and ultimately supporting the development of more durable coffee rust resistant cultivars.

13643703, 2026, 9, Downloaded from https://bsppjournals.onlinelibrary.wiley.com/doi/10.1111/mpp.70341 by Cochrane Colombia, Wiley Online Library on [12/11/2026]. See the Terms and Conditions (https://onlinelibrary.wiley.com/terms-and-conditions) on Wiley Online Library for rules of use; OA articles are governed by the applicable Creative Commons License

4 | Experimental Procedures

4.1 | Cloning of *Hemileia vastatrix* Effector Candidates

Candidate effector sequences (*HvEC*s) lacking the predicted N-terminal signal peptide were amplified by PCR from cDNA prepared from coffee (*C. arabica* 'Catuaí Vermelho IAC-44') leaves infected with *H. vastatrix* race II, the most widespread physiological race of the pathogen (Talhinhas et al. 2017), or from germinated urediniospores as previously described (Maia, Badel, Marin-Ramirez, et al. 2017). *HvEC* sequences had been previously predicted and deposited in GenBank under accession numbers KX670432–KX670525. Primer sequences are listed in Table S3.

PCR products were initially cloned into the Gateway entry vector pENTR/D-TOPO (Invitrogen) and subsequently recombined into the pEDV6 destination vector (Fabro et al. 2011) using Gateway LR Clonase II (Invitrogen), according to the manufacturer's instructions, to generate constructs for delivery through the *P. fluorescens* EtHAn Type III secretion system. For subcellular localization assays, *HvEC* sequences lacking both the signal peptide encoding region and the stop codon were amplified using gene-specific primers and recombined into the binary vector pK7FWG2 (Karimi et al. 2002), generating C-terminal GFP fusion constructs under the control of the CaMV 35S promoter. The integrity and reading frame of all pEDV6::*HvEC* and pK7FWG2::*HvEC-GFP* constructs were confirmed by Sanger sequencing.

4.2 | Bacterial Strains and Growth Conditions

Escherichia coli DH5α was used for routine plasmid construction. Triparental mating was performed to mobilize pEDV6::*HvEC* constructs into *P. fluorescens* EtHAn using *E. coli* HB101 carrying pRK2013 as the helper strain. The empty pEDV6 vector was maintained in *E. coli* DB3.1. EtHAn transformants were selected on Luria Bertani (LB) medium supplemented with chloramphenicol (30 $\mu g\,mL^{-1}$) and gentamicin (25 $\mu g\,mL^{-1}$).

For transient expression assays, *Agrobacterium tumefaciens* GV3101 (pMP90) carrying pK7FWG2::*HvEC-GFP* constructs was grown on LB medium supplemented with rifampicin (100 $\mu g\,mL^{-1}$), gentamicin (25 $\mu g\,mL^{-1}$) and spectinomycin (125 $\mu g\,mL^{-1}$).

4.3 | PTI Suppression Assay

PTI suppression assays were performed essentially as described by Badel et al. (2013) with minor modifications. Suspensions of *P. fluorescens* EtHAn carrying pEDV6::*HvEC* constructs or the empty pEDV6 vector were adjusted to 2×10^7 CFU mL^{-1} in 10 mM $MgCl_2$ and infiltrated into fully expanded leaves of 4- to 5-week-old *N. benthamiana* plants using a needle-free syringe. Seven hours later, an overlapping region was infiltrated with Pto DC3000 at 3×10^6 CFU mL^{-1} to trigger HR.

HR development was evaluated macroscopically 3 days after infiltration. HvECs were classified as PTI suppressors when they reproducibly restored tissue viability within the overlapping infiltration zone compared with the empty vector control. PTI suppression was quantified as the percentage of infiltration sites exhibiting induction of HR relative to the total number of infiltrated sites. Three independent biological experiments were performed, each comprising eight biological replicates, resulting in a total of 24 biological replicates ($n = 24$; Table S1).

Cell death was further confirmed by trypan blue staining. Leaf tissues collected 3 days after infiltration were immersed in trypan blue–lactophenol solution, briefly heated to boiling, incubated for 2 h at room temperature and subsequently cleared in chloral hydrate solution until complete removal of chlorophyll. Stained tissues were examined using bright-field microscopy.

4.4 | Quantification of Pto DC3000 Proliferation

To validate PTI suppression independently of HR scoring, bacterial growth assays were performed following the protocol of Badel et al. (2013) with minor modifications. Leaves were first infiltrated with *P. fluorescens* EtHAn carrying either the empty pEDV6 vector or individual pEDV6::HvEC constructs at 5×10^6 CFU mL^{-1}. Seven hours later, overlapping regions were infiltrated with Pto DC3000 at 1×10^5 CFU mL^{-1}.

Leaf discs (1 cm diameter) were collected immediately after inoculation (0 h) and at 48, 72 and 96 h post-infiltration from three independent plants. Samples were homogenized in 10 mM $MgCl_2$, serially diluted and plated onto King's B medium supplemented with the appropriate antibiotics. Bacterial populations were quantified by enumeration of colony-forming units (CFU).

4.5 | ETI Suppression Assay

Suppression of ETI was evaluated using the AvrB/RPM1 recognition system as previously described (Innes et al. 1993; Kessens et al. 2014). Equal volumes of *P. fluorescens* EtHAn carrying pVSP6::*AvrB* and *Pf* EtHAn carrying either pEDV6::*HvEC* constructs or the empty pEDV6 vector were mixed to obtain a final bacterial concentration of 2×10^7 CFU mlL^{-1} and co-infiltrated into fully expanded *N. benthamiana* leaves.

HvECs were classified as ETI suppressors when they consistently suppressed or substantially attenuated AvrB-induced HR in more than 50% of infiltrated sites across independent experiments. ETI suppression was quantified as the percentage of infiltration sites exhibiting complete or partial suppression of HR relative to the total number of infiltration sites. HR development was evaluated visually and confirmed by trypan blue staining. Three independent experiments with eight biological replicates each were performed ($n = 24$; Table S2).

13643703, 2026, 9, Downloaded from https://bsppjournals.onlinelibrary.wiley.com/doi/10.1111/mpp.70341 by Cochrane Colombia, Wiley Online Library on [12/11/2026]. See the Terms and Conditions (https://onlinelibrary.wiley.com/terms-and-conditions) on Wiley Online Library for rules of use; OA articles are governed by the applicable Creative Commons License

4.6 | Electrolyte Leakage Assay

Electrolyte leakage was used as an independent quantitative measure of ETI-associated cell death following Block et al. (2014) with minor modifications. Five leaf discs (8 mm diameter) from each treatment were transferred to 5 mL of sterile deionized water and incubated for 30 min at room temperature with gentle shaking. The incubation solution was subsequently replaced with fresh deionized water, and conductivity was measured at regular intervals from 0 to 28 h after infiltration using a conductivity meter (mCA-150; MS Tecnopon Instrumentação Científica). Conductivity values ($\mu S\,cm^{-1}$) were used as an indirect estimate of membrane damage associated with ETI-induced cell death. Treatment effects were assessed descriptively based on the separation between mean conductivity values and their standard errors across the time course.

4.7 | RT-qPCR Analysis of *HvEC* Expression During Coffee Infection

Temporal expression profiles of selected HvEC genes were determined by RT-qPCR using RNA samples previously obtained from the compatible interaction between *H. vastatrix* race II and *C. arabica* 'Catuaí Vermelho IAC-44', as described by Maia, Badel, Fernandes, et al. (2017). Samples comprised dormant urediniospores, germinated urediniospores and infected leaf tissues collected at 12, 24, 48 and 72 h, and 9 and 15 days post-inoculation, thereby encompassing the major developmental transitions of the fungal infection cycle.

Total RNA extraction, cDNA synthesis and quality assessment were performed as previously described (Maia, Badel, Marin-Ramirez, et al. 2017). Gene-specific primers used for RT-qPCR are listed in Table S4. Amplification reactions were carried out using a 7500 Real-Time PCR System (Applied Biosystems) with SYBR Green chemistry. Each reaction contained cDNA equivalent to 20 ng of total RNA and was performed in technical duplicate using three independent biological replicates. Cycling conditions consisted of an initial denaturation at 95°C for 10 min followed by 40 amplification cycles of 95°C for 15 s and 60°C for 30 s. Amplification specificity was verified by dissociation curve analysis (60°C–95°C), and primer amplification efficiencies, determined from standard curves, ranged from 92% to 100%, satisfying the requirements for comparative expression analyses.

Relative transcript abundance was calculated using the $2^{-\Delta C_t}$ method (Livak and Schmittgen 2001). Expression levels of each *HvEC* gene were normalized against the geometric mean of three previously validated *H. vastatrix* reference genes: *glyceraldehyde-3-phosphate dehydrogenase* (*HvGAPDH*), *cytochrome c oxidase subunit III* (*HvCytIII*) and *β-tubulin* (*Hvβ-tub*) (Fernandez et al. 2012). RT-qPCR analyses were performed using three biological replicates. For each biological replicate, qPCRs were carried out in duplicate (technical replicates), and the C_t values of the two technical replicates were averaged before calculating relative transcript abundance.

4.8 | Subcellular Localization of HvECs

Subcellular localization of HvEC proteins was investigated by transient expression of C-terminal GFP fusion proteins in *N. benthamiana* leaf epidermal cells using *A. tumefaciens*-mediated transformation. Overnight cultures of *A. tumefaciens* GV3101 (pMP90) carrying pK7FWG2::*HvEC-GFP* constructs were harvested by centrifugation (5000 *g*, 5 min), washed and resuspended in infiltration buffer containing 10 mM $MgCl_2$ and 150 μM acetosyringone.

To determine intracellular localization, *HvEC-GFP* constructs were co-infiltrated (1:1 ratio) with well-established organelle markers fused to mCherry. Nuclear localization was assessed using AtWWP1-mCherry (Silva et al. 2015), whereas plastid localization was evaluated using the tobacco RuBisCO small subunit fused to mCherry (Dabney-Smith et al. 1999). Final bacterial suspensions were adjusted to 4×10^7 CFU mL^{-1} before infiltration into fully expanded leaves of 3-week-old *N. benthamiana* plants.

Fluorescence signals were examined 48 h after agroinfiltration using a Zeiss LSM510 META laser-scanning confocal microscope. GFP fluorescence was excited at 488 nm using an argon laser and detected at 500–550 nm. mCherry fluorescence was excited with a helium-neon laser at 543 nm and detected between 560 and 615 nm. Images were processed using the Zeiss LSM software, and subcellular localization was assigned only when GFP fluorescence consistently colocalized with the corresponding organelle marker in independent biological replicates.

Author Contributions

Thiago Maia: conceptualization, methodology, validation, supervision, writing – original draft, investigation. **Gustavo Marin-Ramirez:** methodology, validation. **Maicon N. Araujo:** methodology, validation. **Larissa G. Zanardo:** writing – review and editing. **Sérgio H. Brommonschenkel:** conceptualization, writing – review and editing, funding acquisition, supervision.

Acknowledgements

We are grateful to Jonathan D. G. Jones for providing the pEDV6 vector and to Narayana M. Upadhyaya for generously supplying the *Pseudomonas fluorescens* EtHAn strain. We also thank all members of the Laboratory of Genetics and Genomis of Host-pathogen Interactions (LG^2IP^2) for valuable discussions and technical support throughout this study.

Conflicts of Interest

The authors declare no conflicts of interest.

Data Availability Statement

The data that support the findings of this study are available on request from the corresponding author.

References

Ahmed, M. B., K. C. G. D. Santos, I. B. Sanchez, et al. 2018. "A Rust Fungal Effector Binds Plant DNA and Modulates Transcription." *Scientific Reports* 8: 14718.

13643703, 2026, 9, Downloaded from https://bsppjournals.onlinelibrary.wiley.com/doi/10.1111/mpp.70341 by Cochrane Colombia, Wiley Online Library on [12/11/2026]. See the Terms and Conditions (https://onlinelibrary.wiley.com/terms-and-conditions) on Wiley Online Library for rules of use; OA articles are governed by the applicable Creative Commons License

Badel, J. L., S. J. Piquerez, D. Greenshields, et al. 2013. "In Planta Effector Competition Assays Detect *Hyaloperonospora arabidopsidis* Effectors That Contribute to Virulence and Localize to Different Plant Subcellular Compartments." *Molecular Plant–Microbe Interactions* 26: 745–757.

Block, A., T. Y. Toruno, C. G. Elowsky, et al. 2014. "The *Pseudomonas syringae* Type III Effector Hopd1 Suppresses Effector-Triggered Immunity, Localizes to the Endoplasmic Reticulum, and Targets the *Arabidopsis* Transcription Factor NTL9." *New Phytologist* 201: 1358–1370.

Brenes, E. G., L. Zambolim, D. P. de Almeida, P. M. Ribeiro, B. Mariz, and E. T. Caixeta. 2025. "Assisted Stacking of Fungal Disease Resistance Genes in Central American Coffee Cultivars." *Agronomy* 15: 230.

Cabral, P. G. C., E. M. Zambolim, L. Zambolim, T. P. Lelis, A. S. Capucho, and E. T. Caixeta. 2009. "Identification of a New Race of *Hemileia vastatrix* in Brazil." *Australasian Plant Disease Notes* 4: 129–130.

Castro, I. S. L., R. R. M. Barreiros, A. O. Mendes, et al. 2022. "Gene Expression and Interactome Analysis of Candidate Effectors Associated With Pre- and Post-Haustorial *Hemileia vastatrix*–Coffee Interaction." *Journal of Biotechnology and Biomedicine* 5: 198–213.

Cheng, Y., K. Wu, J. Yao, et al. 2017. "Pstha5a23, a Candidate Effector From the Obligate Biotrophic Pathogen *Puccinia striiformis* f. sp. *tritici*, Is Involved in Plant Defense Suppression and Rust Pathogenicity." *Environmental Microbiology* 19: 1717–1729.

Crabill, E., A. Joe, A. Block, J. M. van Rooyen, and J. R. Alfano. 2010. "Plant Immunity Directly or Indirectly Restricts the Injection of Type III Effectors by the *Pseudomonas syringae* Type III Secretion System." *Plant Physiology* 154: 233–244.

Dabney-Smith, C., P. W. Van Den Wijngaard, Y. Treece, W. J. Vredenberg, and B. D. Bruce. 1999. "The C Terminus of a Chloroplast Precursor Modulates Its Interaction With the Translocation Apparatus and PIRAC." *Journal of Biological Chemistry* 274: 32351–32359.

Fabro, G., J. Steinbrenner, M. Coates, et al. 2011. "Multiple Candidate Effectors From the Oomycete Pathogen *Hyaloperonospora arabidopsidis* Suppress Host Plant Immunity." *PLoS Pathogens* 7: e1002348.

Feng, F., F. Yang, W. Rong, et al. 2012. "A *Xanthomonas* Uridine 5′-Monophosphate Transferase Inhibits Plant Immune Kinases." *Nature* 485: 114–118.

Fernandez, D., E. Tisserant, P. Talhinhas, et al. 2012. "454-Pyrosequencing of *Coffea arabica* Leaves Infected by the Rust Fungus *Hemileia vastatrix* Reveals In Planta-Expressed Pathogen-Secreted Proteins and Plant Functions in a Late Compatible Plant–Rust Interaction." *Molecular Plant Pathology* 13: 17–37.

Figueroa, M., D. Ortiz, and E. C. Henningsen. 2021. "Tactics of Host Manipulation by Intracellular Effectors From Plant Pathogenic Fungi." *Current Opinion in Plant Biology* 62: 102054.

Henningsen, E. C., C. Langlands-Perry, E. A. Stone, P. N. Dodds, M. Figueroa, and J. Sperschneider. 2025. "Genome Biology of Rust Fungi." *Annual Review of Phytopathology* 63: 529–552.

Innes, R. W., S. R. Bisgrove, N. M. Smith, A. F. Bent, B. J. Staskawicz, and Y. C. Liu. 1993. "Identification of a Disease Resistance Locus in *Arabidopsis* That Is Functionally Homologous to the *RPG1* Locus of Soybean." *Plant Journal* 4: 813–820.

Jones, D. A. B., and S. Raffaele. 2025. "Phytopathogen Effector Biology in the Burgeoning AI Era." *Annual Review of Phytopathology* 63: 63–88.

Karimi, M., D. Inzé, and A. Depicker. 2002. "GATEWAY Vectors for *Agrobacterium*-Mediated Plant Transformation." *Trends in Plant Science* 7: 193–195.

Kemen, E., A. C. Kemen, M. Rafiqi, et al. 2005. "Identification of a Protein From Rust Fungi Transferred From Haustoria Into Infected Plant Cells." *Molecular Plant–Microbe Interactions* 18: 1130–1139.

Kessens, R., T. Ashfield, S. H. Kim, and R. W. Innes. 2014. "Determining the GmRIN4 Requirements of the Soybean Disease Resistance Proteins Rpg1b and Rpg1r Using a *Nicotiana glutinosa*-Based Agroinfiltration System." *PLoS One* 9: e108159.

Kleemann, J., L. J. Rincon-Rivera, H. Takahara, et al. 2012. "Sequential Delivery of Host-Induced Virulence Effectors by Appressoria and Intracellular Hyphae of the Phytopathogen *Colletotrichum higginsianum*." *PLoS Pathogens* 8: e1002643.

Li, G., M. Newman, H. Yu, et al. 2024. "Fungal Effectors: Past, Present, and Future." *Current Opinion in Microbiology* 81: 102526.

Li, Y., X. Qu, W. Yang, et al. 2025. "A Fungal Pathogen Suppresses Host Leaf Senescence to Increase Infection." *Nature Communications* 16: 2864.

Livak, K. J., and T. D. Schmittgen. 2001. "Analysis of Relative Gene Expression Data Using Real-Time Quantitative PCR and the 2−ΔΔCT." *Methods* 25: 402–408.

Lorrain, C., K. C. Gonçalves dos Santos, H. Germain, A. Hecker, and S. Duplessis. 2019. "Advances in Understanding Obligate Biotrophy in Rust Fungi." *New Phytologist* 222: 1190–1206.

Maia, T., J. L. Badel, M. B. Fernandes, C. A. D. Bragança, E. S. G. Mizubuti, and S. H. Brommonschenkel. 2017. "Variation in Aggressiveness Components in the *Hemileia vastatrix* Population in Brazil." *Journal of Phytopathology* 165: 174–188.

Maia, T., J. L. Badel, G. Marin-Ramirez, et al. 2017. "The *Hemileia vastatrix* Effector HvEC-016 Suppresses Bacterial Blight Symptoms in Coffee Genotypes With the *SH1* Rust Resistance Gene." *New Phytologist* 213: 1315–1329.

Maia, T., H. V. S. Rody, R. G. H. Bombardelli, T. G. Souto, L. E. A. Camargo, and C. B. Monteiro-Vitorello. 2022. "A Bacterial Type Three Secretion-Based Delivery System for Functional Characterization of *Sporisorium scitamineum* Plant Immune Suppressing Effector Proteins." *Phytopathology* 112: 1513–1523.

Ngou, B. P. M., P. Ding, and J. D. G. Jones. 2022. "Thirty Years of Resistance: Zig-Zag Through the Plant Immune System." *Plant Cell* 34: 1447–1478.

Ngou, B. P. M., R. Heal, M. Wyler, M. W. Schmid, and J. D. G. Jones. 2022. "Concerted Expansion and Contraction of Immune Receptor Gene Repertoires in Plant Genomes." *Nature Plants* 8: 1146–1152.

Nguyen, H. P., S. Chakravarthy, A. C. Velásquez, et al. 2010. "Methods to Study PAMP-Triggered Immunity Using Tomato and *Nicotiana benthamiana*." *Molecular Plant–Microbe Interactions* 23: 991–999.

Nirmala, J., T. Drader, X. Chen, B. Steffenson, and A. Kleinhofs. 2010. "Stem Rust Spores Elicit Rapid RPG1 Phosphorylation." *Molecular Plant–Microbe Interactions* 23: 1635–1642.

Nirmala, J., T. Drader, P. K. Lawrence, et al. 2011. "Concerted Action of Two Avirulent Spore Effectors Activates *Reaction* to *Puccinia graminis 1* (*Rpg1*)-Mediated Cereal Stem Rust Resistance." *Proceedings of the National Academy of Sciences of the United States of America* 108: 14676–14681.

Nomura, H., T. Komori, S. Uemura, et al. 2012. "Chloroplast-Mediated Activation of Plant Immune Signaling in *Arabidopsis*." *Nature Communications* 3: 926.

Ozketen, A. C., M. Cetinturk, C. Rampitsch, et al. 2026. "The Proteome Study of Germinated *Puccinia triticina* Urediniospores Reveals a Novel Effector Protein Required for Virulence." *Scientific Reports* 16: 15726.

Pan, Q., Y. Zhang, Y. Yang, et al. 2025. "The *Puccinia striiformis* Effector Pst11215 Manipulates Mitochondria to Suppress Host Immunity by Promoting TaVDIP1-Mediated Ubiquitination of TaVDAC1." *New Phytologist* 244: 1961–1978.

Petre, B., D. L. Joly, and S. Duplessis. 2014. "Effector Proteins of Rust Fungi." *Frontiers in Plant Science* 5: 416.

13643703, 2026, 9, Downloaded from https://bsppjournals.onlinelibrary.wiley.com/doi/10.1111/mpp.70341 by Cochrane Colombia, Wiley Online Library on [12/11/2026]. See the Terms and Conditions (https://onlinelibrary.wiley.com/terms-and-conditions) on Wiley Online Library for rules of use; OA articles are governed by the applicable Creative Commons License

Petre, B., C. Lorrain, D. G. Saunders, et al. 2016. "Rust Fungal Effectors Mimic Host Transit Peptides to Translocate Into Chloroplasts." *Cellular Microbiology* 18: 453–465.

Porto, B. N., E. T. Caixeta, S. M. Mathioni, et al. 2019. "Genome Sequencing and Transcript Analysis of *Hemileia vastatrix* Reveal Expression Dynamics of Candidate Effectors Dependent on Host Compatibility." *PLoS One* 14: e0215598.

Qi, M., T. I. Link, M. Müller, et al. 2016. "A Small Cysteine-Rich Protein From the Asian Soybean Rust Fungus, *Phakopsora pachyrhizi*, Suppresses Plant Immunity." *PLoS Pathogens* 12: e1005827.

Qi, T., J. Guo, P. Liu, et al. 2019. "Stripe Rust Effector PstGSRE1 Disrupts Nuclear Localization of ROS-Promoting Transcription Factor TaLOL2 to Defeat ROS-Induced Defense in Wheat." *Molecular Plant* 12: 1624–1638.

Ramachandran, S. R., C. Yin, J. Kud, et al. 2017. "Effectors From Wheat Rust Fungi Suppress Multiple Plant Defense Responses." *Phytopathology* 107: 75–83.

Redditt, T. J., E.-H. Chung, H. Z. Karimi, et al. 2019. "AvrRpm1 Functions as an ADP-Ribosyl Transferase to Modify NOI-Domain Containing Proteins, Including *Arabidopsis* and Soybean RPM1-Interacting Protein4." *Plant Cell* 31: 2664–2681.

Rocafort, M., I. Fudal, and C. H. Mesarich. 2020. "Apoplastic Effector Proteins of Plant-Associated Fungi and Oomycetes." *Current Opinion in Plant Biology* 56: 9–19.

Sera, G. H., C. H. S. de Carvalho, J. C. de Rezende Abrahão, et al. 2022. "Coffee Leaf Rust in Brazil: Historical Events, Current Situation, and Control Measures." *Agronomy* 12: 496.

Silva, M. C., L. Guerra-Guimarães, I. Diniz, et al. 2022. "An Overview of the Mechanisms Involved in Coffee–*Hemileia vastatrix* Interactions: Plant and Pathogen Perspectives." *Agronomy* 12: 326.

Silva, M. C., M. Nicole, L. Guerra-Guimarães, and C. J. Rodrigues Jr. 2002. "Hypersensitive Cell Death and Posthaustorial Defence Responses Arrest the Orange Rust (*Hemileia vastatrix*) Growth in Resistant Coffee Leaves." *Physiological and Molecular Plant Pathology* 60: 169–183.

Silva, M. C., M. Nicole, L. Rijo, J. P. Geiger, and C. J. Rodrigues Jr. 1999. "Cytochemical Aspects of the Plant-Rust Fungus Interface During the Compatible Interaction *Coffea arabica* (cv. Caturra)–*Hemileia vastatrix* (Race III)." *International Journal of Plant Sciences* 160: 79–91.

Silva, P. A., J. C. Silva, H. D. Caetano, et al. 2015. "Comprehensive Analysis of the Endoplasmic Reticulum Stress Response in the Soybean Genome: Conserved and Plant-Specific Features." *BMC Genomics* 16: 783.

Sowden, R. G., S. J. Watson, and P. Jarvis. 2018. "The Role of Chloroplasts in Plant Pathology." *Essays in Biochemistry* 62: 21–39.

Talhinhas, P., H. G. Azinheira, B. Vieira, et al. 2014. "Overview of the Functional Virulent Genome of the Coffee Leaf Rust Pathogen *Hemileia vastatrix* With an Emphasis on Early Stages of Infection." *Frontiers in Plant Science* 5: 88.

Talhinhas, P., D. Batista, I. Diniz, et al. 2017. "The Coffee Leaf Rust Pathogen *Hemileia vastatrix*: One and a Half Centuries Around the Tropics." *Molecular Plant Pathology* 18: 1039–1051.

Thomas, W. J., C. A. Thireault, J. A. Kimbrel, and J. H. Chang. 2009. "Recombineering and Stable Integration of the *Pseudomonas syringae* pv. *syringae* 61 *hrp/hrc* Cluster Into the Genome of the Soil Bacterium *Pseudomonas fluorescens* Pf0-1." *Plant Journal* 60: 919–928.

Vargas-Guevara, C., C. Vargas-Segura, J. Villalta-Villalobos, L. F. P. Pereira, and A. Gatica-Arias. 2018. "A Simple and Efficient Agroinfiltration Method in Coffee Leaves (*Coffea arabica* L.): Assessment of Factors Affecting Transgene Expression." *3 Biotech* 8: 471.

Xu, N., X. Luo, W. Li, Z. Wang, and J. Liu. 2017. "The Bacterial Effector AvrB-Induced RIN4 Hyperphosphorylation Is Mediated by a Receptor-Like Cytoplasmic Kinase Complex in *Arabidopsis*." *Molecular Plant–Microbe Interactions* 30: 502–512.

Xu, Q., C. Tang, X. Wang, S. Sun, J. Zhao, and Z. Kang. 2019. "An Effector Protein of the Wheat Stripe Rust Fungus Targets Chloroplasts and Suppresses Chloroplast Function." *Nature Communications* 10: 5571.

Yuan, M., Z. Jiang, G. Bi, et al. 2021. "Pattern-Recognition Receptors Are Required for NLR-Mediated Plant Immunity." *Nature* 592: 105–109.

Zheng, L., J. Yao, F. Gao, et al. 2016. "The Subcellular Localization and Functional Analysis of Fibrillarin2, a Nucleolar Protein in *Nicotiana benthamiana*." *BioMed Research International* 2016: 2831287.

Supporting Information

Additional supporting information can be found online in the Supporting Information section. **Figure S1:** AvrB activates effector-triggered immunity (ETI) in *Nicotiana benthamiana*. Leaves (4–5 weeks old) were infiltrated with *Pseudomonas fluorescens* EtHAn expressing pVSP6::AvrB construction (white dotted circle) and *P. fluorescens* EtHAn carrying pEDV6 empty (red dotted circle) suspensions at 1×10^7 CFU mL^{-1}. The hypersensitive response (HR) was scored at 48 h after infiltrations. Picture shows *N. benthamiana* leaf stained with trypan blue to visualize cell death. **Figure S2:** Transient expression of two *Hemileia vastatrix* effector candidate fusion proteins (HvEC_028-GFP and HvEC_101-GFP) showing nonspecific accumulation patterns in *Nicotiana benthamiana* leaf cells. Bacterial suspensions of *Agrobacterium tumefac* GV3101 (pMP90) carrying *HvEC*-GFP fusion constructions and same strain carrying AtWWWP1-mcherry fusion construct were co-infiltrated (1:1 ratio) to a final concentration of 4×10^7 CFU mL^{-1} into *N. benthamiana* leaf cells. About 72 h after co-infiltrations, leaf disks were sampled and viewed by confocal microscopy. GFP and mCherry were excited at 488 and 561 nm, respectively. GFP (green) and mCherry (red) fluorescence were collected at 505–525 and 580–620 nm, respectively. Scale bars = 50 μm. **Figure S3:** Subcellular localization pattern of free GFP expressed in *Nicotiana benthamiana* leaf cells. Bacterial suspensions of *Agrobacterium tumefaciens* GV3101 (pMP90) carrying the expression construct encoding GFP alone (pK7EGFP) and same strain carrying the nuclear marker AtWWWP1-mcherry fusion were co-infiltrated (1:1 ratio) to a final of 4×10^7 CFU mL^{-1} into *N. benthamiana* leaves. About 72 h post-agroinfiltration, leaf explants were excised and GFP patterns were examined in epidermal cells by confocal microscopy. Scale bars = 10 μm. **Table S1:** Selected group of *Hemileia vastatrix* candidate effectors (HvECs) tested for PTI-suppressing activity in *Nicotiana benthamiana*. **Table S2:** Selected group of *Hemileia vastatrix* candidate effectors (HvECs) tested for ETI-suppressing activity in *Nicotiana benthamiana*. **Table S3:** Primer sequences used for cloning *Hemileia vastatrix* effector genes (HvECs) for the Effector Detector Vector system assay. **Table S4:** Sequences of primers for seven *Hemileia vastatrix* effector candidate genes (HvECs) used for RT-qPCR.

13643703, 2026, 9, Downloaded from https://bsppjournals.onlinelibrary.wiley.com/doi/10.1111/mpp.70341 by Cochrane Colombia, Wiley Online Library on [12/11/2026]. See the Terms and Conditions (https://onlinelibrary.wiley.com/terms-and-conditions) on Wiley Online Library for rules of use; OA articles are governed by the applicable Creative Commons License